Progress In Electromagnetics Research C, Vol. 33, 109–121, 2012

DESIGN OF LEAKY WAVE ANTENNA WITH COMPOSITE RIGHT-/LEFT-HANDED TRANSMISSION LINE STRUCTURE FOR CIRCULAR POLARIZATION RADIATION

M. Ishii[1], T. Fukusako[1, *], and A. Alphones[2]

[1]Graduate School of Science and Technology, Kumamoto University, 2-39-1 Kurokami, Chuo-ku, Kumamoto 860-8555, Japan

[2]School of Electrical and Electronic Engineering, Nanyang Technological University, 50 Nanyang Avenue, Singapore 639798, Singapore

Abstract—This paper presents a design procedure for the generation of circular polarization (CP) from the composite right/left handed (CRLH) transmission line (TL) with a coupled inter-digit structure and an inductive stub. The E_x and E_y components are generated from the parallel stubs and the fingers, respectively. The 90°-phase difference can be obtained by optimizing the dimension of the unit cell. In addition, the suitable amplitude ratio of $|E_x|$ and $|E_y|$ for CP generation is obtained by selecting a suitable position of the CRLH-TL between both edges of the ground. As a result, a CP with a measured bandwidth of 30.5% for an axial ratio (AR) of < 3 dB in the boresight direction is obtained. Using the behavior in both the left-handed (LH) and right-handed (RH) frequency regions, a scanning angle of the main beam of approximately 30° can be obtained by varying the frequency between 2.58 GHz and 2.99 GHz. Furthermore, the principle of CP generation is discussed.

1. INTRODUCTION

Leaky wave antenna (LWA) that uses a composite right/left-handed transmission line (CRLH-TL) has been investigated by numerous researchers [1–12]. The radiation in the right-handed (RH) frequency with parallel phase and group velocities is directed in the forward propagating direction. However, the radiation in the left-handed (LH) frequency with anti-parallel phase and group velocities is directed in

Received 21 August 2012, Accepted 20 September 2012, Scheduled 3 October 2012

* Corresponding author: Takeshi Fukusako (fukusako@cs.kumamoto-u.ac.jp).

the backward propagating direction. Therefore, backward-to-endfire frequency scanning (BEFS) is available by sweeping the frequency between the RH and LH frequencies. BEFS with a CRLH-TL was first demonstrated experimentally in [3] and was discussed in [4]. Various LWAs with BEFS have since been proposed and discussed in various transmission line configurations [8–12]. The radiation angle from the antenna depends on the ratio between the phase constant of transmission line and the wave number in free space. Although BEFS behavior can be applied to radars and sensors, most of the previous LWAs with a CRLH-TL are linearly polarized. An LWA that can generate CP has recently been presented in [10]. This structure requires two LWAs and a phase shifter for generating two orthogonal polarizations that are 90° out of phase.

A single-element circularly polarized LWA having a CRLH-TL structure was presented by some of the authors [13]. In this paper, the design procedure, the principle for generating CP and the antenna behavior are discussed in detail. One key to generate CP is the L-shaped structure of a stub and the inter-digit structure of a unit cell, both of which should be designed considering the dispersion characteristics and the 90° phase difference between E_x and E_y since the orthogonal components of E_x and E_y are generated from the stub and the fingers, respectively. The 90°-phase difference is obtained by optimizing the fingers (see Fig. 1(a)). Another key is to control the ratio of $|E_x|$ and $|E_y|$ by choosing a suitable position of the LWA element transmission line between the two edges of the ground plane so as to effectively take advantage of the effect of radiation from the edges. As such, in the present study, the axial ratio (AR) characteristics and a brief explanation of the physical behavior is presented. Finally, the dependence of the radiation pattern on frequency is discussed.

2. ANTENNA STRUCTURE

The structure of a unit cell and the equivalent circuit of the proposed antenna are shown in Figs. 1(a) and 1(b), respectively. The unit cell consists of a ground plane, a dielectric, a feeding microstrip line, fingers (a coupled inter-digit structure), and an inductive parallel stub with a shorted termination through a via ($\phi = 0.5\,\mathrm{mm}$) to the ground plane. This structure has a serial inductance L_R, a parallel capacitance C_R, and a conventional RH-TL, as well as a parallel inductance L_L and a series capacitance C_L for a LH medium. The fingers give the C_L, and the parallel stub gives the L_L. Fig. 1(c) shows the LWA discussed here with a comb-shaped TL of eight unit cells on a dielectric substrate. The transmission direction of the TL is parallel to y-axis.

A Taconic substrate of TLY-5CH/CH with a dielectric constant of 2.2, a $\tan\delta$ of 0.001, and a thickness of 1.6 mm was used for this structure, which had a ground plane with dimensions of 97.4 mm $\times$ 50 mm $\times$ 0.035 mm. In this paper, the ground plane width was fixed to 50 mm which has been optimized for the lowest AR characteristics in the operation band around 3 GHz. On the other hand, the unit cell has finger length l_c and stub length l_s, both of which have been optimized as 9 mm and 10.1 mm, respectively, considering both the 90° phase difference between $|E_x|$ and $|E_y|$ for CP and the suitable dispersion characteristics for this frequency region. The gap g between the stub and the fingers is also optimized as 0.8 mm, where the width w of a finger has been chosen as 0.35 mm. Furthermore, the intervals between the fingers are 0.3 mm.

This LWA is fed from the $-y$ direction (left edge) of the microstrip line, and the microstrip line at the right edge is terminated by an impedance of 50 Ω because the TL is basically designed to have a characteristic impedance of 50 Ω. The TL element of the LWA is initially placed on the ground plane so that the center position of the stub is located at the center of the ground plane in the x direction.

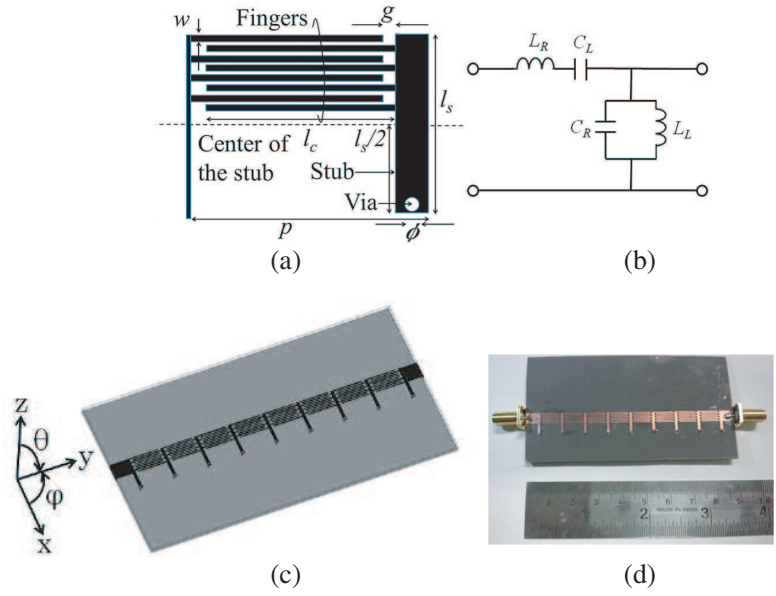

Figure 1. (a) Structure of the unit cell [1]. (b) Equivalent circuit of the unit cell [1]. (c) Basic structure of the comb-shaped LWA using a CRLH-TL. (d) Photo of the fabricated antenna.

3. DESIGN AND SIMULATION RESULTS

To understand the dispersion characteristics and also for parametric studies, the simulations were conducted using Ansoft HFSS 13.0. From the S-parameters in the simulations, the dispersion diagram is obtained considering the transmission theory in the priodic structure [1].

In this section, the dispersion characteristics for a unit cell are first discussed. The effects of the dimensions of both the stub and the finger are then presented. Finally, the effect of the position on the ground plane is discussed.

3.1. Dispersion Characteristics

Figure 2 shows the dispersion characteristics of the unit cell. A small band gap of 50 MHz (1.8% at 2.74 GHz), where the β is very close to zero in the dispersion diagram, should be allowed to exist from 2.71 GHz to 2.76 GHz since the finger dimension should be modified from the design for the zero-band-gap to obtain the 90°-phase difference between E_x and E_y with the widest 3-dB AR bandwidth. Considering that βp ($\beta = 2\pi/\lambda$: phase constant, p: length of the unit cell in the y direction) should be lower than that of the free space for a leaky wave to occur, the frequency for LH behavior is from 2.18 GHz to 2.71 GHz. Similarly, the frequency for RH behavior is from 2.76 GHz to 4.24 GHz. On Fig. 2, the discontinuity in the dispersion curve around 3.5 GHz is caused by the self-resonance of the fingers [2].

3.2. Parametric Studies on the Dimensions of the Stub and the Fingers

The effects of the finger length and the stub on the AR characteristics are shown in Figs. 3(a) and 3(b), respectively. Fig. 3(a) shows the dependence of the AR characteristics on l_c for fixed l_s at 10.1 mm, and

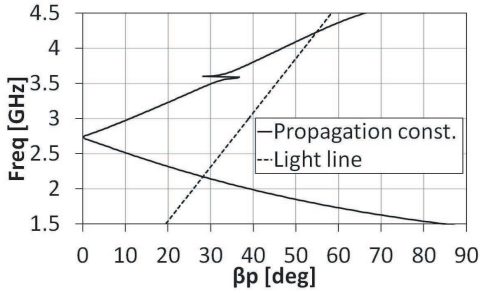

Figure 2. Dispersion diagram.

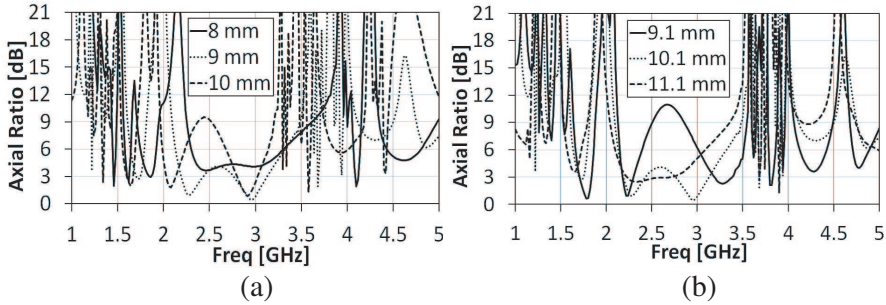

Figure 3. Dependence of axial ratio characteristics for $\phi = \theta = 0$ on (a) the length of the finger l_c and (b) the length of the stub l_s.

Fig. 3(b) shows the dependence of the AR characteristics on l_s from 9.1 to 11.1 mm for fixed l_c at 9 mm. Based on these results, it is clearly seen that the dimensions of the stub and the fingers strongly affect the AR.

3.3. Parametric Study on the Position on the Ground Plane

The length of the fingers and stubs are 9 mm and 10.1 mm, respectively. The AR characteristics of the LWA with CRLH-TL is investigated when the element position is shifted by 8 mm in the $+x$ direction. As shown in Fig. 4, a bandwidth of 32.7% for an AR of < 3 dB is obtained when the LWA element is shifted. The AR bandwidth is widened because the electric field in the x direction are mainly changed by the shift, and so have almost an equal strength in the AR frequency band. In order to explain this behavior, Fig. 5(a) show the distribution of E_x in the z-x plane at 2.9 GHz. The E_x distribution is close to symmetrical for both the left and right half of the figure. This indicates the E_x is weak in the far field since the electric field to both $\pm x$ directions cancel out each other. On the other hand, for the 8-mm shift to $+x$ direction, E_x is concentrated between the element and the right edge of the ground plane as shown in Fig. 5(b), whereas the field strength around the left edge of the ground is reduced. As a result, as shown in Fig. 6, the 8-mm TL shift yields almost the equal amplitude of E_x and E_y in the far field around 2.9 GHz. In addition to the equal amplitude, the phase difference of around 90° between E_x and E_y is comfirmed in Fig. 7. This 8-mm shift can improve the phase difference to be close to -90 degrees as well as the amplitude ratio. As a result of the above condition, CP is generated as shown in Fig. 4. Furthermore, current behavior on the ground plane is discussed here. Figs. 8(a) and 8(b) show the current distributions on the ground for shifts of 0 mm and

8 mm, respectively. Compared to the 0-mm shift, the current for the 8-mm shift is concentrated between the stub and the ground edge, since the current from the element is reflected by the discontinuity of edge in x direction. This behavior leads to enhance the E_x component.

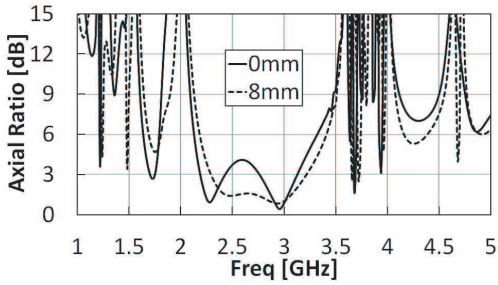

Figure 4. Variation in AR characteristics while shifting the LWA element in the x direction from the initial position.

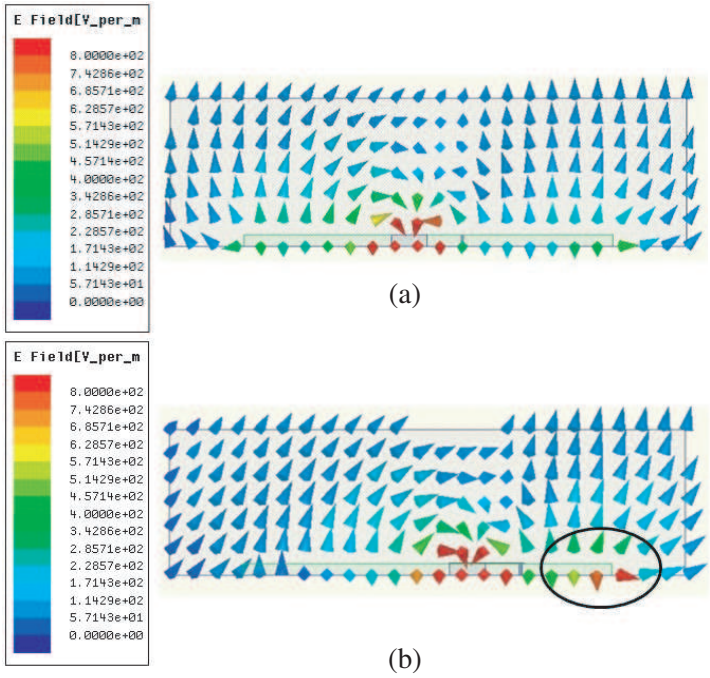

Figure 5. Electric field distribution at 2.9 GHz in the z-x plane with shifts by (a) 0 mm and (b) 8 mm from the initial position in the $+x$ direction.

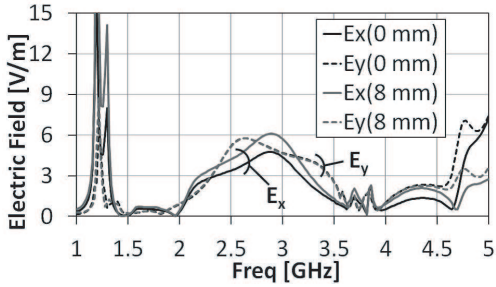

Figure 6. Dependence of electric field E_x and E_y on the TL shift.

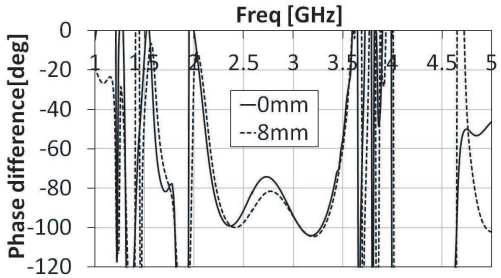

Figure 7. Dependence of the phase difference on the TL shift.

In order to generate a CP, a phase difference of 90° is required for the orthogonal modes. In this structure, the phase difference is caused by the current on the fingers and the stub for generating E_x and E_y, respectively, as determined primarily by the dimensions of the fingers and the stub length. Therefore, such an L-shaped structure generates a phase difference by traveling-wave-like excitation. A CP antenna based on a similar principle is discussed in [14]. To explain this behavior, Fig. 9 shows the current distribution on the CRLH-TL at 2.9 GHz when the CRLH-TL is located on the center of the ground plane. Fig. 9(a) shows the current distribution at 0 degree and the strong current is mainly on the fingers. However, the current distribution at 90 degrees shown in Fig. 9(b) has strong current on the stubs. Therefore, the 90 degrees phase difference by the L-shaped structure composed of the fingers and the stub contributes to the generation of CP. However, the dimensions also affect the dispersion characteristics. Hence, the band gap between 2.71 GHz and 2.76 GHz should exist for the present design, as mentioned in Subsection 3.1.

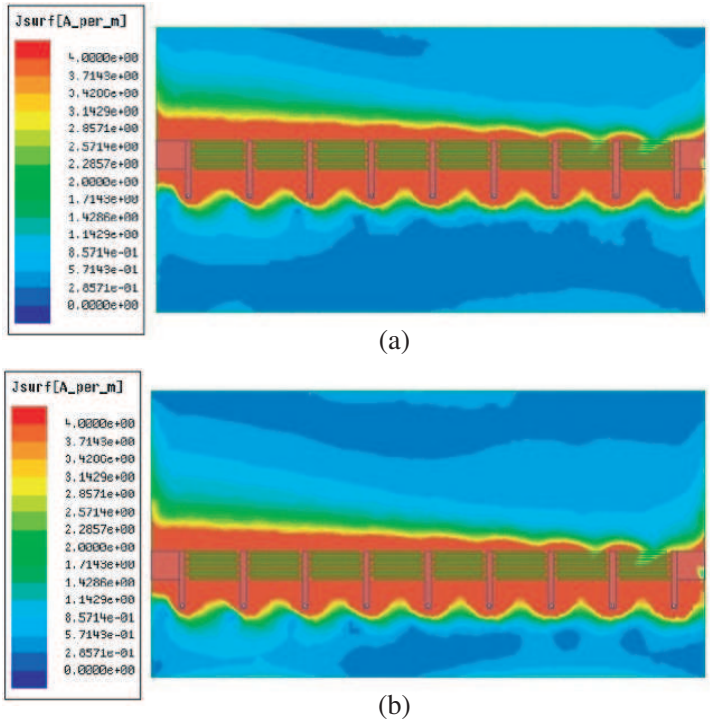

Figure 8. Current distribution at 2.9 GHz with shifts by (a) 0 mm and (b) 8 mm from the initial position in the $+x$ direction.

4. EXPERIMENTAL RESULTS

The proposed antenna design with $l_s = 10.1$ mm, $l_c = 9$ mm, and a shift of the element by 8 mm was fabricated and measured. The fabricated antenna is shown in Fig. 1(d). Fig. 10 shows both the simulated and measured S_{11} and S_{21} characteristics. The estimated radiation efficiency characteristics is obtained in Fig. 11 by applying the equation, $1 - |S_{11}|^2 - |S_{21}|^2$ [11]. The slight discrepancy between the simulated and measured results are due to the fabrication errors and the assumed substrate electrical parameters. This slight difference causes the difference in simulated and measured radiation efficiency in Fig. 11. However, the available S_{11} characteristics cover the frequencies for both the LH/RH regions with a radiation efficiency of more than 20%, which is in a valid range for this conventional TL structure since the present structure has not been optimized for an antenna but a transmission line. However the low radiation efficiency could be

improved by increasing the number of unit cells because the increased TL length can improve power leakage [12].

For generating CP, a small band gap of 50 MHz (1.8%) has been allowed to exist so as to keep the widest AR bandwidth. The calculated Bloch impedance assuming periodicity should be theoretically zero in

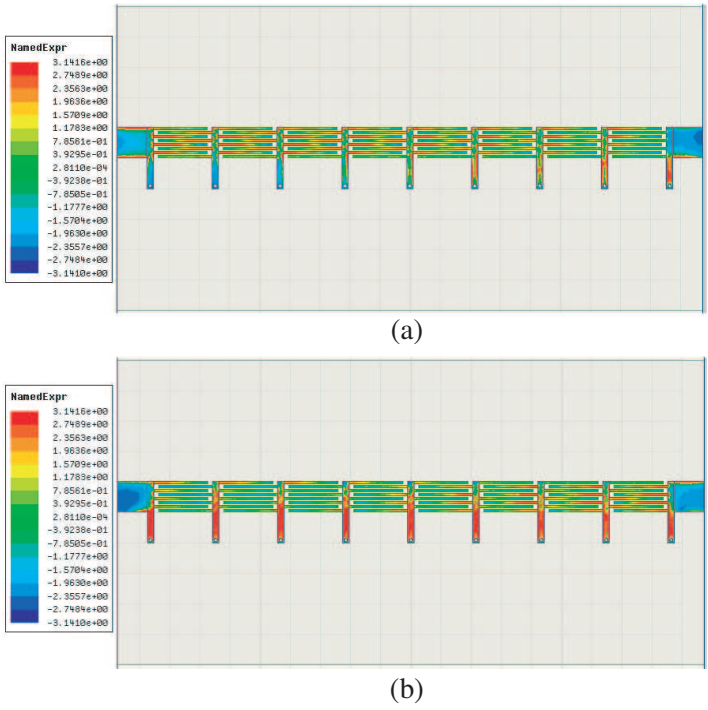

Figure 9. Current distribution at (a) 0 degree (reference) and (b) 90 degrees. The operating frequency is 2.9 GHz.

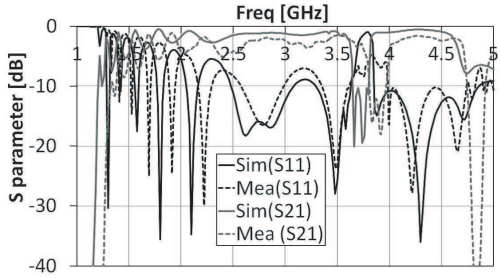

Figure 10. Simulated and measured S_{11} and S_{21} characteristics.

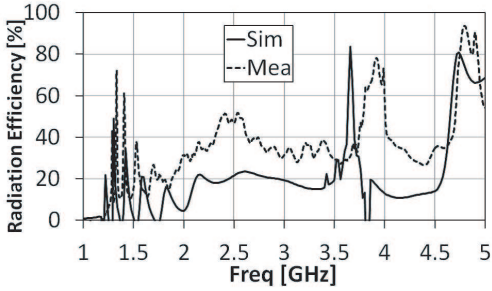

Figure 11. Variation in the simulated and measured radiation efficiency.

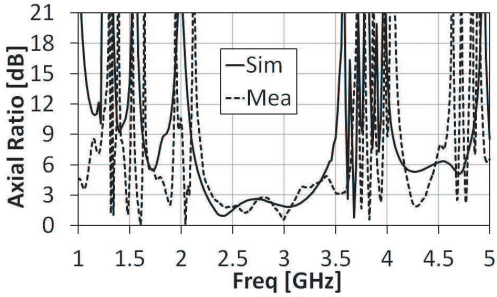

Figure 12. AR characteristics for the simulation and the measurement.

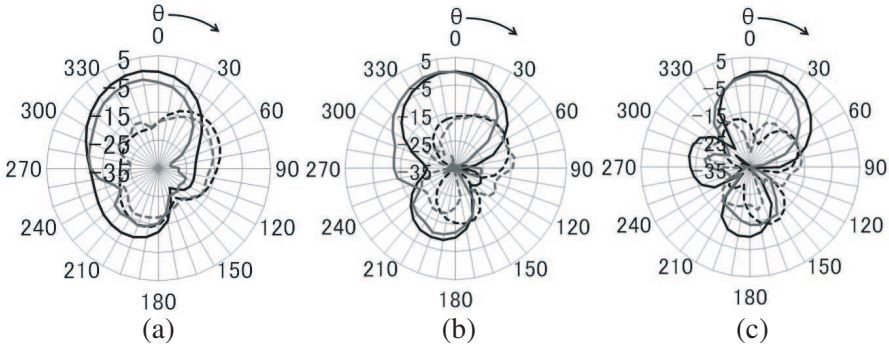

Figure 13. Simulated and measured radiation patterns on the y-z plane at (a) 2.58 GHz, (b) 2.74 GHz, and (c) 2.99 GHz. The units of the radial axes are dBic.Solid black line: Simulated LHCP, Solid gray line: Measured LHCP, Dashed black line: Simulated RHCP, Dashed gray line: Measured RHCP.

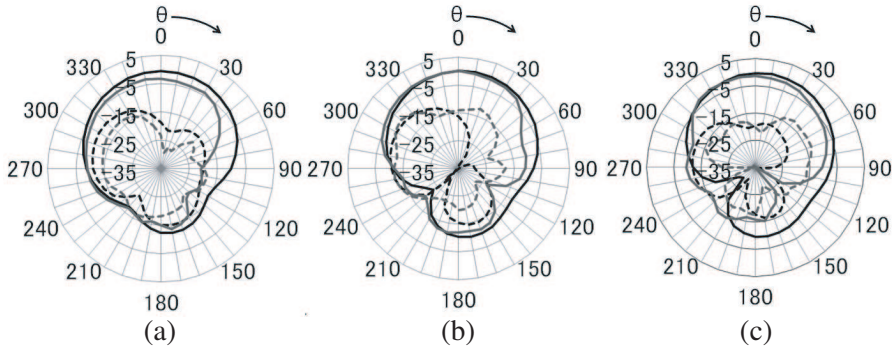

Figure 14. Simulated and measured radiation patterns on the z-x plane at (a) 2.58 GHz, (b) 2.74 GHz, and (c) 2.99 GHz. The units of the radial axes are dBic. Solid black line: Simulated LHCP, Solid gray line: Measured LHCP, Dashed black line: Simulated RHCP, Dashed gray line: Measured RHCP.

the band gap. On the other hand, the available impedance matching can be practically obtained with the widest 3-dB AR bandwidth according to the Fig. 10. One of the reasons of the contradiction is that the number of unit cell is very small for the periodic structure. Another reason is that attenuation of the leaky wave has not been considered in the calculation process [1]. As a result, the band gap of 1.8% is so small that the Bloch impedance is not varied largely with frequency in the band gap. Therefore, the LH and RH behaviors can be obtained, although the variation in β with frequency could be small.

Figure 12 shows the AR characteristics in the $+z$ direction. A 3-dB AR band is observed in the bore-sight direction ($+z$) around the band gap frequency (2.71 GHz–2.76 GHz). Figs. 13 and 14 show the radiation patterns on the y-z and z-x planes, respectively, at (a) 2.58 GHz (LH region), (b) 2.74 GHz (band gap region), and (c) 2.99 GHz (RH region). Seeing from the antenna in the propagation direction, the CP is defined as RHCP (Right-Hand CP) when the rotating direction of electric field is clockwise. These figures reveal fair agreement between the simulated and measured results with sufficient cross-polarization discrimination (XPD) of more than 15 dB for an AR of 3 dB. However, no scanning in the z-x plane is observed. As a result, a CP scanning of 30° is obtained by varying the frequency between 2.58 GHz and 2.99 GHz. Furthermore, the CP sense does not change in either the LH or RH region. The antenna gain is approximately 1 dBic. However, the antenna gain can be enhanced as the number of unit cells increases.

5. CONCLUSION

We have presented a detail design procedure for CP-LWA with a CRLH-TL structure and effects of each process in this procedure using full-wave simulations and experiments. For a design to generate CP, we can allow to have a small band gap between the LH and RH region to keep 90°-phase difference. And the position of the CRLH-TL is shifted to $+x$ direction to obtain the same amplitude between E_x and E_y which are generated from the stubs and the fingers, respectively. As a result, the proposed LWA with CRLH-TL is available for CP radiation in the backward, forward and the normal direction with the same CP sense. On the other hand, the present structure should be modified for increasing the radiation efficiency. However, the basic principle discussed in this paper is available for radars and sensor systems, which need beam scanning and CP instead of conventional LWAs.

REFERENCES

1. Caloz, C. and T. Itoh, *Electromagnetic Metamaterials*, Willey-Interscience, 2006.
2. Hashemi, M. R. and T. Itoh, "Dual-mode leaky-wave excitation in symmetric composite right/left-handed structure with center vias," *IEEE MTT-S International Microwave Symposium Digest*, 9–12, Anaheim, USA, May 2010.
3. Liu, L., C. Caloz, and T. Itoh, "Dominant mode (DM) leaky-wave antenna with backfire-to-endfire scanning capability," *Electronics Letters*, Vol. 38, No. 23, 1414–1416, Nov. 2002.
4. Caloz, C. and T. Itoh, "Novel microwave devices and structures based on the transmission line approach of meta-materials," *IEEE MTT-S International Microwave Symposium Digest*, Vol. 1, 195–198, 2003.
5. Cheng, J., A. Alphones, and M. Tsutsumi, "Double periodic composite right/left handed transmission line and its applications to leaky wave antennas," *IEEE Transactions on Antennas and Propagation*, Vol. 59, 3679–3686, Oct. 2011.
6. Cheng, J., A. Alphones, and L. C. Ong, "Broadband leaky wave antenna based on composite right/left handed substrate integrated waveguide," *Electronics Letters*, Vol. 46, No. 24, 1584–1585, Nov. 2010.
7. Kang, M., C. Caloz, and T. Itoh, "Miniaturized MIM CRLH transmission line structure and application to backfire-to-endfire

leaky-wave antenna," *IEEE Antennas and Propagation Society International Symposium*, Vol. 1, 827–830, 2010.

8. Losito, O., M. Gallo, V. Dimiccoli, D. Barletta, and M. Bozzetti, "A tapered design of a CRLH-TL leaky wave antenna," *Proceedings of the 5th European Conference on Antennas and Propagation, (EUCAP)*, 357–360, 2011.
9. Dong, Y. and T. Itoh, "Composite right/left-handed substrate integrated waveguide and half mode substrate integrated waveguide leaky-wave structure," *IEEE Transactions on Antennas and Propagation*, Vol. 59, 767–775, 2011.
10. Hashemi, M. R. and T. Itoh, "Circularly polarized composite right/left-handed leaky wave antenna," *IEEE International Conference Wireless Information Technology and System, (ICWITS)*, 1–4, 2010.
11. Cheng, J. and A. Alphones, "Leaky-wave radiation behavior from a double periodic composite right/left-handed substrate integrated waveguide," *IEEE Transactions on Antennas and Propagation*, Vol. 60, 1727–1735, 2012.
12. Anghel, A. and R. Cacoveanu, "Improved composite right/left-handed cell for leaky-wave antenna," *Progress In Electromagnetics Research Letters*, Vol. 22, 59–69, 2011.
13. Ishii, M. and T. Fukusako, "Circularly polarized leaky wave antenna using composite right/left-handed transmission line," *PIERS Proceedings*, 972–975, Moscow, Russia, Aug. 19–23, 2012.
14. Joseph, R., S. Nakao, and T. Fukusako, "Broadband square slot antenna for polarization with separated l-probes and stubs in the slot," *IEICE Trans. Communication*, Vol. E94-B, No. 04, 951–959, Apr. 2011.